Developmentally Guided Ego-Exo Force Discrimination for a Humanoid Robot

Aaron Edsinger-Gonzales
MIT Computer Science Artificial Intelligence Lab
Cambridge, Ma.
edsinger@csail.mit.edu

Abstract

We present an approach for discriminating between forces a humanoid robot induces on itself (ego) and forces arising from its interaction with the environment (exo). The method uses the correlation of the interaction forces between the arms to determine whether the robot is touching itself, or an external agent is interacting with the arm. The ability is realized in a series of developmental stages as an initial step towards a robot body schema which is grounded in physical sensorimotor experiences. The approach has been evaluated on a bimanual upper-torso humanoid named Domo.

1. Introduction

Humans are not able to tickle themselves. While this is perhaps fortunate, it indicates that our brains learn to discriminate between proprioceptive sensations induced by the environment and those that are generated by ourselves. The reason for this is not clear, but it has been suggested that the efference-copy mechanism in the cerebellum is responsible for attenuating the effects of the tickling (Blakemore et al., 2000). This mechanism allows us to delineate external perceptual stimuli from those which are a consequence of our own action. The term "ego-exo discrimination" is used to describe this mechanism. It is a biologically significant ability, providing us with the ability to recognize self-generated limb movements as our own, to filter optic flow due to egomotion and stabilize our visual image, and to predict the sensory consequences of our own actions.

We present a developmentally guided method for ego-exo discrimination on a humanoid robot based purely on the its proprioceptive sense of force. The discriminator is constructed over a series of semi-autonomous developmental stages. Using an efference copy mechanism based on a forward model of the manipulator dynamics, the robot is able to discriminate between forces which are a natural result of a ballistic reach, forces which are generated from human-robot interaction, and forces due to physical coupling between its arms.

Figure 1: *These experiments were conducted on the robot Domo. It has compliant, force sensing actuators in its arms and hands which allow it to safely explore its environment and its own body.*

Ego-exo discrimination can be seen as a basic underpinning in the formulation the "ecological self" (Bermudez et al., 1995). The ecological self is a physically embodied representation of the self, derived from the direct relationships between the body and its environment. The representation is constructed through explorations and interactions in the world. It is our position that on a robot, an ecological self should be be constructed over time, according to a developmental plan. Early, simple exploratory behaviors can generate the sensorimotor experiences necessary to scaffold further stages in the construction. One step in such a developmental approach for

a humanoid robot is to incorporate, at the lowest level, the notion of ego-exo discrimination.

(Rochat, 1998) has conducted experiments with neonates to pin down a developmental course for ego-exo discrimination. His work suggests that infants are born with the means to discriminate themselves from the world. A 2-3 month old infant will explore the intermodal sensory relationships of its body through self-exploration. Babbling provides an opportunity to relate vocal cord vibration with auditory feedback. A newborn infant will spend up to 20% of his time touching his face with his hands. This is an intermodal event, where both the face and the hand experience sensory stimulation. This type of self-exploration, especially with the hands, begins at around 3 months and is dominant in the first year.

Experiments in ego-exo discrimination, both in robotics and developmental psychology, typically involve vision and audition. For example, (Gross et al., 1999), learned the visual ego-motion of a Khepera robot, while (Michel et al., 2004) learned the characteristic time-delay between an action and its visual perception as a signal used in self-recognition. (Yoshikawa et al., 2004) visually discriminated between the robot body and the world based on the visual texture invariance of the body.

In contrast, the work described here uses strictly the robot's sense of force as a discrimination cue. When the robot moves its arms about, its proprioceptive stream will include force components from the manipulator mass dynamics, the motor torques, gravitational loading, robot-human interaction, and bimanual coupling. The following sections presents a method for discriminating the source of these forces. This represents a preliminary step in developing the robot's ecological self.

2. Methodology

2.1 The Robot Platform

This work was developed on an upper torso humanoid robot named Domo, developed by the author. Domo, pictured in Figure 1 has 29 active degrees of freedom (DOF), 58 proprioceptive sensors, and 24 tactile sensors. Of these, 22 DOF use force controlled and compliant actuators. There are two six DOF force controlled arms, two four DOF force controlled hands, a two DOF force controlled neck, and a seven DOF active vision head. The real-time sensorimotor system is managed by an embedded network of DSP controllers. The vision system includes two FireWire CCD cameras. The cognitive system runs on a small, networked cluster of PCs.

Domo's manipulator characteristics are analogous to human manipulators which are very good at controlling forces, but relatively poor at controlling joint position

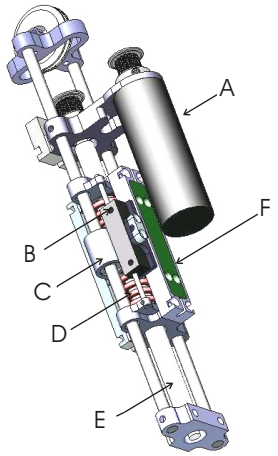

Figure 2: *The Series Elastic Actuator (SEA) used throughout the robot provides natural compliance and high-fidelity force sensing and control. A brushless DC motor (A) imparts a linear motion to the inner drive carriage (C) through a precision ballscrew (E). The inner drive carriage transmits motion to the outer drive carriage (F) through two springs (D). The deflection of the springs is measured with a linear potentiometer (B), providing a force-feedback signal.*

(Gomi and Kawato, 1997). The 14 Series Elastic Actuators (SEA) (Pratt and Williamson, 1995) and 8 Force Sensing Compliant actuators (FSC)(Edsinger-Gonzales, 2004) provide natural compliance in the robot limbs as well as high-fidelity force-sensing and control. The actuators incorporate a compliant element (spring) between the motor output and the driven joint. The deflection of the spring, being proportional to the torque at the joint, is measured and used as a force-feedback signal in a $1Khz$ control loop. Domo's naturally compliant force-control allows it to safely interact with humans and with itself. This is a critical ability given the experiments presented here, where the robot is to actively engage in contact exploration over a long period of time. We refer the reader to (Edsinger-Gonzales and Weber, 2004) for further technical details on the robot.

2.2 Force model

Forces exerted on the arm during movement and those occurring from interaction with the environment appear identical to the first order. Discrimination between these forces requires additional contextual information which can be provided by kinematic and dynamic models of the arm.

An epigenetic approach to robotics suggests that

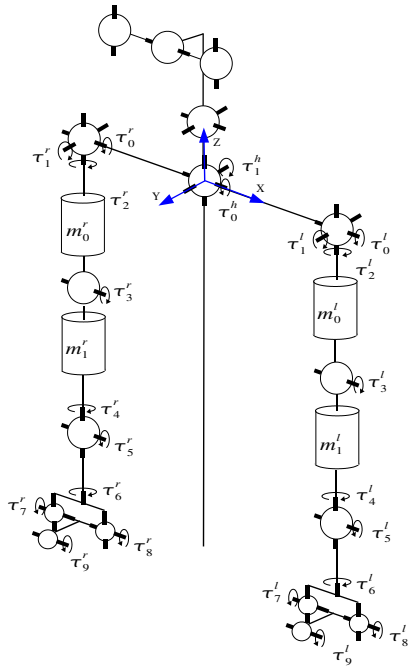

Figure 3: *The kinematic structure of the robot used in the force model. Each arm and hand has 10 force controlled joints,* $\{\tau_0, ...\tau_9\}$. *This work uses only the first four joints of each arm,* $\tau^l = \{\tau_0^l, \tau_1^l, \tau_2^l \tau_3^l\}$ *and* $\tau^r = \{\tau_0^r, \tau_1^r, \tau_2^r \tau_3^r\}$. *The joint angles, not pictured, are* q^l *and* q^r. *The force model simplifies the mass of each arm as* $m = \{m_0, m_1\}$.

the forward and inverse kinematics and dynamics of the arm should be learned autonomously, allowing online adaptation to changes in limb length and mass as the robot, or organism, grows. This is a significant learning challenge which has fostered a large body of research. (Schaal and Atkeson, 1994) demonstrated learning a dynamic model for a juggling task, and (Sun and Scassellati, 2004) recently developed an autonomous approach to learning a manipulator's forward kinematics using a radial basis function network.

Autonomous learning of the kinematics and dynamics of the robot is beyond the scope of this work. Instead, a simplified kinematic model and dynamic model is constructed by hand. The robot dynamics and kinematics are illustrated in Figure 3. The angles and torques of the first four joints of each arm are represented by $q = \{q_0, q_1, q_2, q_3\}$ and $\tau = \{\tau_0, \tau_1, \tau_2 \tau_3\}$. The left and right arms are distinguished as t^l, q^l and t^r, q^r when necessary. The mass of each arm is modeled as a point mass for the upper and lower links as $m = \{m_0, m_1\}$.

The model contains the following components.

1 Forward kinematics. The forward kinematics model maps from joint space q to cartesian space x. It provides the manipulator Jacobian J and, consequently, the instantaneous force at the hand ($f_h = J\tau$). The joint torques caused by a force at the hand is also known ($\tau = J^T f_h$) (Craig, 1989).

2 Force model. The instantaneous torques acting on the manipulator are decomposed as follows:

- τ: the sensed torque
- τ_{Dyn}: the dynamic torque caused by mass accelerations
- τ_{Grav}: the torque from gravitational loading
- τ_{Mot}: the torque generated by the motor
- τ_{Exo}: external interaction torques
- τ_{Ego}: bimanual coupling interaction torques
- $\tau = \tau_{Dyn} + \tau_{Mot} + \tau_{Ego} + \tau_{Exo} + \tau_{Grav}$

The goal is to determine when $\tau_{Ego} \neq 0$ during bimanual force coupling and when $\tau_{Exo} \neq 0$ during human-robot interaction and other interactions with the world.

3 Inverse dynamics. The joint-space form of the inverse dynamics is: $\tau = M(q)\ddot{q} + V(q, \dot{q}) + G(q)$. The term $M(q)\ddot{q}$ represents the torques due to mass accelerations. $V(q, \dot{q})$ represents the centrifugal and Coriolis torque. $G(q)$ is the torque due to gravity. A full dynamic model requires complete knowledge of the mass distribution of the arms which can be difficult to obtain and calibrate. For ego-exo discrimination, which only requires an approximate prediction of the forces, it is sufficient to assume that $V(q, \dot{q}) = 0$ and to ignore inertial effects by using point masses in $M(q)$. Consequently, $\tau_{Dyn} = M(q)\ddot{q}$ and $\tau_{Grav} = G(q)$ can be easily computed using a recursive Newton-Euler formulation(Gourdeau, 2005).

3. Developmental Stages

Domo's motor and perceptual abilities are to be incrementally expanded over a series of developmental stages, where latter stages can leverage off of previous ones. The developmental program executes on a behavior based architecture which provides semi-autonomous execution. Each new stage can be dynamically brought on-line in real-time.

The developmental course for human infants provides a useful reference for incorporating ego-exo discrimination into Domo. Kinesthetic feedback is involved in motor patterns as early as the prenatal stage, where the fetus can express coordinated movements during spontaneous action patterns (Robinson and Kleven, 2004). The action patterns occur in a constrained environment, allowing an early proprioceptive sense of the body. The infant is unable to reach to objects at birth, but after

one week will attempt directed arm movements. Motor plans at this stage are largely reflex driven ballistic movements which enable a motor exploration and learning phase. At three months the infant will reach for objects of interest, but it is not until two years of age that the kinematics parameters involved in arm control assume adult levels (Konczak et al., 1997).

The developmental plan for Domo begins with building an adaptive model of the resting proprioceptive state of the robot. A subsequent human guided exploration phase circumscribes the allowable manipulator workspace. The robot then engages in a workspace exploration stage. In this stage, ballistic reaching allows for an efference copy model of arm torques to be built. The model provides the necessary substrate on which to build ego-exo discrimination. The modules of the developmental plan are illustrated in Figure 4.

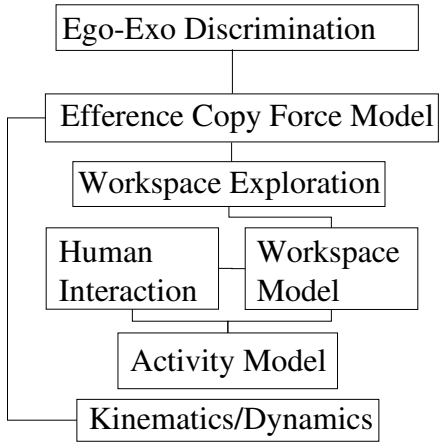

Figure 4: *The ego-exo development plan. The robot starts with an approximate kinematic and dynamics model. An activity model signals the occurrence of any proprioceptive activity. Human interaction with the arms allow the robot to continually model the kinematic workspace online. As the workspace model forms, ballistic reaching movements within the workspace allows for manipulator force exploration. An efference-copy model is then constructed which generates the force expectation during the ballistic exploration. This model is able to signal when ego-exo forces are present. Final discriminators determine if the forces are ego or exo based.*

3.1 Adaptive activity model

Domo's development begins by remaining at rest with its arms at its sides. An activity model is constructed which signals proprioceptive disturbances caused by other behaviors acting on the motors or by human interaction. Assuming a Gaussian model of the sensor noise at rest, an online Gaussian estimator is used to characterize the time derivative of each proprioceptive sensor's resting state. After an initial bootstrap stage, the robot is allowed to move. A simple discriminator signals the level of robot activity based on it's probability of being at rest. The activity model is updated when the robot is at rest to accommodate drift in the sensor characteristics.

3.2 Workspace exploration through human-robot interaction

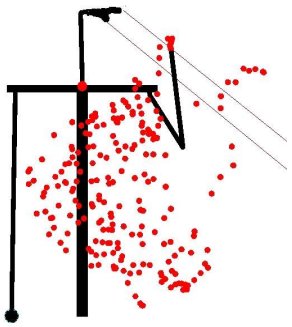

Figure 5: *A graphical display of the workspace model for one arm.*

In this stage of development the robot engages in exploratory ballistic movements in order to generate the sensorimotor experiences required to enable ego-exo discrimination.

The dynamic model predicts the torques induced by gravity as τ_{Grav}. Knowing τ_{Grav} allows the arms to be placed in a zero-gravity mode where they effectively cancel out gravitational loading and float in-place. This allows a human to guide the arms safely about their workspace while the activity model signals the workspace model when to capture the kinematic trajectories of the manipulators.

The workspace model provides the robot with a set of joint configurations assumed to be appropriate poses for human style interaction and manipulation. An exploration behavior runs on each of Domo's arms. It periodically picks a random joint pose from those available in the workspace model. The arm reaches towards the pose using a virtual spring controller running on top of the zero-gravity force control loop (Edsinger-Gonzales and Weber, 2004). The inherent compliance of the arms and controller allows for safe exploration of its workspace during this phase. Figure 5 illustrates the workspace model after 1 minute of human interaction.

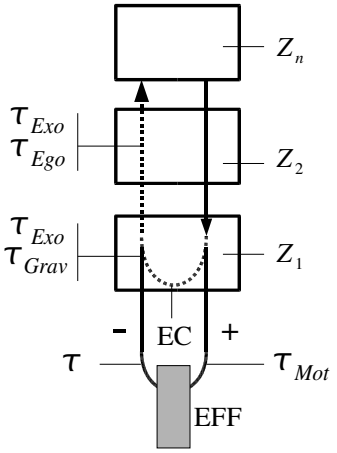

Figure 6: The efference copy mechanism for ego-exo discrimination (adapted from von Holst's original schematic of the reafference principle (von Holst and Mittelstae, 1973)). Descending brain centers $Z_n - Z_1$ have sensorimotor connections to a motor effector, EFF. The action generated by motor command, τ_{Mot}, generates the reafferent sensory signal τ. The command τ_{Mot} also generates in Z_1 the efferent copy EC, composed of terms $\{\tau_{Dyn}, \tau_{Grav}\}$. The signal is compared to τ and the difference indicates a disturbance force $\{\tau_{Ego}, \tau_{Exo}\}$ which is relayed to the higher brain centers. .

3.3 Efference copy

Efference-copy is a mechanism implicated in the cerebellum (S.J. Blakemore, 2001) which provides a creature with the means to distinguish between self-induced sensory signals and the behaviorally relevant signals generated by the external world. The mechanism predicts the sensory consequence of a motor action using a forward model, and discrepancies between the forward model and the sensory outcome can be amplified for cognitive processing. Ego-exo discrimination can be viewed as an efference copy mechanism. Figure 6 adapts the original formulation of efference copy by (von Holst and Mittelstae, 1973) to indicate how ego-exo discrimination can occur.

The mechanism predicts the sensed torque, τ in the arm induced by the motor command τ_{Mot}. This prediction is based on $\{\tau_{Dyn}, \tau_{Grav}\}$ generated by the force model. An ideal force model would give $\tau_{Ego} + \tau_{Exo} = \tau - \tau_{Mot} - \tau_{Dyn} - \tau_{Grav}$. However, the force model ignores sensor noise, drive-train friction, and higher-order dynamic effects. Fortunately, it is sufficient to discriminate when $\tau_{Ego} + \tau_{Exo}$ is above a threshold. An online Gaussian model captures the error distribution as:

$$\epsilon = \|\tau - \tau_{Mot} - \tau_{Dyn} - \tau_{Grav}\|^2$$
$$P(x) = \frac{1}{\sigma\sqrt{2\pi}} e^{\frac{-(x-\mu)^2}{2\sigma^2}}$$
$$\phi_{Eff} = H(P(\mu + 2\sigma) - P(\epsilon))$$

, where $H(x)$ is the Heaviside step function. ϕ_{Eff} is the discriminator output. Force model errors outside of 2 standard deviations are assumed to be ego-exo induced. The Gaussian distribution is updated continuously at $100Hz$. If the robot experiences continuous ego-exo stimulation, then the distribution will shift such that it habituates to the stimulation over time. Figure 7 shows the output of the efference copy model.

3.4 Ego-exo discrimination

The final development stage discriminates if interaction forces at the hands are internally generated through bimanual coupling, or are externally generated through human-robot interaction. The assumption is made that the interaction forces do not simultaneously have ego and exo components.

Discrimination is performed by noting that ego forces should be correlated across the two arms while exo forces should not. The efference copy prediction error can be formulated in terms of hand forces as

$$e_h^l = J(\tau^l - \tau_{Mot}^l - \tau_{Dyn}^l - \tau_{Grav}^l)$$
$$e_h^r = J(\tau^r - \tau_{Mot}^r - \tau_{Dyn}^r - \tau_{Grav}^r)$$

The error vectors $\{e_h^l, e_h^r\}$ should point in approximately equal and opposite directions during bimanual coupling. In an ideal case, a linear least-squares fit to $\{e_h^l, e_h^r\}$ should give the line slope as $b = -1.0$ and the correlation coefficient as $\rho = 1.0$.

Figure 8a illustrates the least-squares fit of hand force errors during 1 minute of workspace exploration without bimanual coupling. Each of the cartesian directions $[x, y, z]$ are treated identically. This resulted in a fit of $\{b = 0.117, \rho = 0.127\}$, indicating little correlation in the hand forces.

The robot's hands were then artificially coupled together by an elastic band to constrain the robot to experience continuous bimanual coupling of ego forces. Figure 8b illustrates a least-squares fit of $\{b = -0.644, \rho = 0.598\}$ during 1 minute of exploration. These results demonstrate significant correlation during the bimanual coupling phase as expected.

It should be noted that the force errors during bimanual coupling are not continuously correlated. As the two arms move in a coupled motion, the interaction forces can be intermittent. However, the robot does not suddenly switch between ego and exo exploration. These are exploratory phases which have

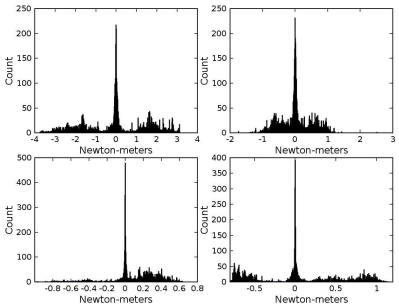

(a)

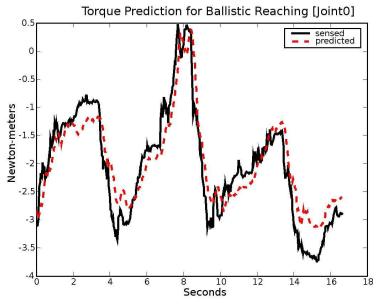

(b)

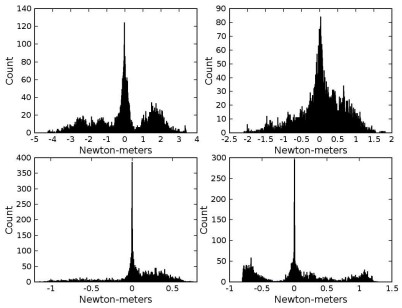

(c)

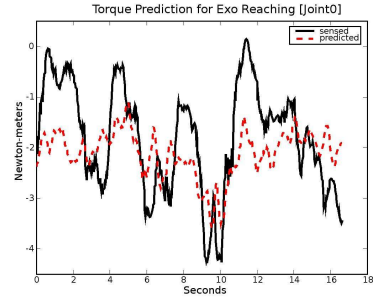

(d)

Figure 7: Efference copy results. For ballistic reaching without ego-exo forces: (a) Prediction error histograms for each joint (Error: $\tau - \tau_{Mot} - \tau_{Dyn} - \tau_{Grav}$) (b) The sensed and predicted torques over time for τ_0^l. For ballistic reaching with ego-exo forces: (c) Prediction error histograms for each joint (d) The sensed and predicted torques.

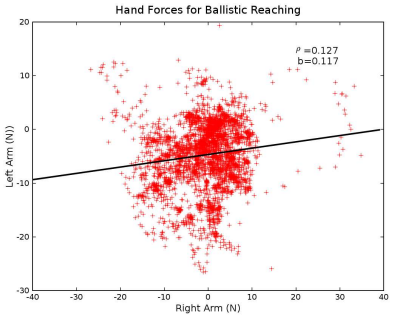

(a)

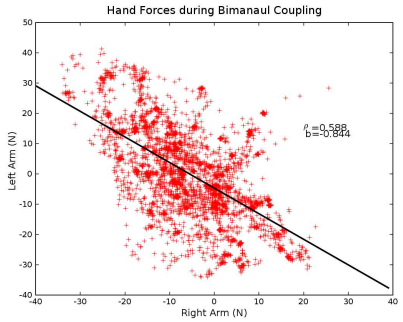

(b)

Figure 8: The bimanual interaction forces at the hands are correlated during self-contact (ego). This is demonstrated by a linear fit to the hand forces during: (a) Ballistic reaching with no self-contact. Correlation coefficient $\rho = .127$, Slope $b = .117$. (b) Reaching with bimanual coupling. Correlation coefficient $\rho = .598$, Slope $b = -0.644$

durations of at least several seconds. A least-squares fit to the errors was found to be susceptible to this intermittent nature as it discards the relative magnitude of the force errors. However, the correlation is also evident in the dot product between $\{e_h^l, -e_h^r\}$, which is large during ego exploration. A more robust ego-exo discrimination can be made as:

$$\eta = -e_h^l \cdot e_h^r$$
$$\phi_{Ego} = H(\eta - \alpha)\phi_{Eff}^l \phi_{Eff}^r$$
$$\phi_{Exo} = (1 - \phi_{Ego})(\phi_{Eff}^l + \phi_{Eff}^r)$$

, with Heaviside function $H(x)$ and threshold parameter α. This final discriminator gives $\phi_{Ego} = 1$ when ego forces exist due to bimanual coupling, $\phi_{Exo} = 1$ when an external agent is applying forces to the manipulator, and $\{\phi_{Ego} = 0, \phi_{Exo} = 0\}$ during normal ballistic reaching. The discriminator output is illustrated in Figure 9.

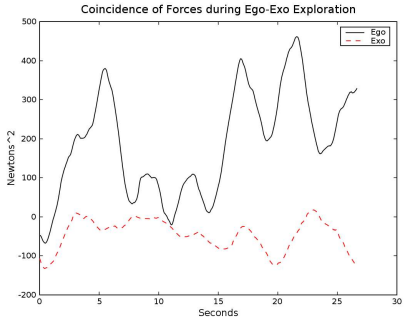

(a)

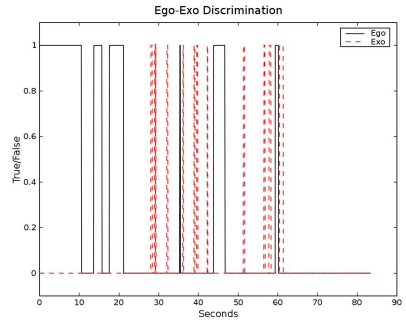

(b)

Figure 9: (a) The coincidence of hand forces (η) during an episode of ego exploration (solid) and ballistic reaching (dotted). (b) The output of the final discriminator. From $[t = 0 : 25]$ the robot is engaged in ego (solid) exploration. From $[t = 25 : 60]$ the robot is doing ballistic reaching with exo (dotted) disturbances. From $[t = 60 : 90]$ the robot is doing ballistic reaching without ego-exo disturbances.

4. Discussion

We have described work in giving a 29 DOF humanoid robot a physically embodied representation of its self which is derived from direct relationships between its body and its environment. The robot is capable of ego-exo discrimination based purely on its proprioceptive sense of force. The discriminator is constructed over a series of semi-autonomous developmental stages. Using an efference copy mechanism based on a forward model of the manipulator dynamics, the robot is able to discriminate between forces that are a natural result of a ballistic reach, forces that are generated from human-robot interaction, and forces due to physical coupling between its arms.

The approach described is broadly applicable to any robot manipulator with force-feedback. However, as described, it is not fully autonomous. The discriminators require hand-tuned thresholds, and as such, lack the adaptivity to be robust under varying conditions. Relatively high threshold values were needed to prevent false-positive discriminations. An adaptive, non-linear discriminator could lower these values and improve the sensitivity of the system. A future direction for this work is to learn the forward dynamic model and discriminators online during the exploration phase.

The sense of force, what it feels like to move and touch ones arms, is an underutilized modality in robotics research. The work described here is a preliminary step towards developing a robot's "ecological self", where the notion of self is as an object distinct from the environment and grounded in real, physical sensorimotor experiences.

References

Bermudez, J., Marcel, A., and Eilan, N., (Eds.) (1995). *The Body and the Self*. The MIT Press, Cambridge, Mass.

Blakemore, Wolpert, and Frith (2000). Why can't you tickle yourself? *NeuroReport*, 1(11).

Craig, J. (1989). *Introduction to Robotics*. Addison Wesley, 2 edition.

Edsinger-Gonzales, A. (2004). Design of a Compliant and Force Sensing Hand for a Humanoid Robot. In *Proceedings of the International Conference on Intelligent Manipulation and Grasping*.

Edsinger-Gonzales, A. and Weber, J. (2004). Domo: A Force Sensing Humanoid Robot for Manipulation Research. In *Proceedings of the 2004 IEEE International Conference on Humanoid Robots*, Santa Monica, Los Angeles, CA, USA. IEEE Press.

Gomi, H. and Kawato, M. (1997). Human arm stiffness and equilibrium-point trajectory during multi-joint muscle movement. *Biological Cybernetics*, 76:163–171.

Gourdeau, R. (2005). *ROBOOP - A robotics object oriented package in C+*. http://www.cours.polymtl.ca/roboop/.

Gross, Heinze, Seiler, and Stephan (1999). A neural architecture for sensorimotor anticipation. *Neural Networks*.

Konczak, J., Borutta, M., and Dichgans, J. (1997). The development of goal-directed reaching in infants. *Experimental Brain Research*, 113:465–474.

Michel, Gold, and Scassellati (2004). Motion-based robotic self-recognition. In *IEEE/RSJ International Conference on Intelligent Robots and Systems*, Sendai, Japan.

Pratt, G. and Williamson, M. (1995). Series Elastic Actuators. In *Proceedings of the IEEE/RSJ International Conference on Intelligent Robots and Systems (IROS-95)*, volume 1, pages 399–406, Pittsburg, PA.

Robinson, S. and Kleven, G. (2004). *Prenatal development of postnatal functions (Advances in Infancy Research series)*, chapter Learning to move before birth. Greenwood Press, New York.

Rochat, P. (1998). Self-perception and action in infancy. *Experimental Brain Research*, 123:102–109.

Schaal, S. and Atkeson, C. G. (1994). Robot juggling: An implementation of memory-based learning. *Control Systems Magazine*.

S.J. Blakemore, C.D. Frith, D. W. (2001). The cerebellum is involved in predicting the sensory consequences of action. *NeuroReport*, 12(11):1879–1884.

Sun, G. and Scassellati, B. (2004). Reaching through learned forward model. In *IEEE-RAS/RSJ International Conference on Humanoid Robots*, Santa Monica, CA.

von Holst, E. and Mittelstae, H. (1973). *The Behavioural Physiology of Animals and Man: The Collected Papers of Erich von Holst*, chapter The reafference principle. (1950). University of Miami Press, Coral Gables, FL.

Yoshikawa, Y., Tsuji, Y., Hosoda, K., and Asada, M. (2004). Is it my body? body extraction from uninterpreted sensory data based on the invariance of multiple sensory attributes. In *Proceedings of the 2004 IEEE/RSJ International Conference on Intelligent Robots and Systems*.